

Training overdamped dynamics

Marc Berneman and Daniel Hexner

Faculty of Mechanical Engineering, Technion, 320000 Haifa, Israel

In regimes where inertia is negligible, the temporal evolution is governed by overdamped dynamics. This limit is particularly relevant in soft-matter contexts, such as polymers, colloidal suspensions, and processes occurring at the cellular scale. Being able to manipulate the dynamics of such many-particle systems would enable control over rate-dependent elastic responses, time-dependent material properties, relaxation processes, and perhaps the hydrodynamics of suspensions. In this work, we develop a framework for manipulating overdamped dynamics through local, physically motivated update rules. Our approach is inspired by ideas from physical learning and directed aging, in which microscopic parameters adapt autonomously to endow a material with a desired function. Using the Rayleighian formulation, whose minimization reproduces the overdamped equations of motion, we derive approximate directed-aging and equilibrium-propagation rules tailored to dissipative systems. To demonstrate these ideas, we study a disordered Maxwell material that behaves elastically at short times but flows at long times. By locally modifying the viscous damping, we show that one can tune the viscous Poisson's ratio and shape local mechanical responses. These results illustrate how materials can be trained to exhibit targeted rate-dependent elastic and viscous behaviors.

I. INTRODUCTION

Systems in which inertia is negligible are governed by overdamped dynamics, where the velocity of each degree of freedom is proportional to the internal or external forces acting upon it. Such dynamics arise across a wide range of physical, chemical, and biological contexts, including polymers [1], colloidal suspensions [2], cellular and tissue mechanics [3, 4], reaction networks, and even models of collective animal behavior [5]. Despite their apparent simplicity at the level of individual components, overdamped systems can exhibit rich emergent behavior. On macroscopic scales, this behavior is described by hydrodynamics, elasticity, and conductivity. Understanding and predicting these collective phenomena remain central challenges in soft matter physics, materials science, and biological physics.

Beyond prediction, the ability to control overdamped dynamics would enable the design of materials with programmable, time-dependent properties and allow complex physical or biological systems [6, 7] to be endowed with targeted functional responses. Achieving a desired function requires tuning the microscopic interactions. For example, modifying local stiffnesses or the geometry of elastic structures enables control over elastic properties [8–12]; varying interaction affinities allows control over self-assembly [13–16]; and adjusting conductivities yields precise input-output relations in resistor networks [17]. Realizing such control first requires solving an inverse design problem to identify the necessary microscopic parameters, followed by modifying these parameters or fabricating the corresponding structures.

An alternative approach is to employ self-organization to modify material parameters, enabling control over system properties without fabrication or direct manipulation of the microstructure [18–20]. In directed aging [18, 21–23] and physical learning [24–34] frameworks, microscopic interaction parameters evolve autonomously in response to external forcing. Such local evolution may

arise from natural physical processes, including plasticity, viscoelastic relaxation, or damage, or from synthetic update rules relevant to engineered systems. To date, most studies have focused on the quasi-static limit, in which the system remains close to force balance. Extending these ideas to fully dynamical regimes enables access to new classes of systems and responses, including materials actuated at finite rates and, potentially, active systems. Although recent work has developed adaptation rules for undamped and damped Newtonian dynamics [35–40], specialized rules for overdamped systems may be both simpler and more practical in this regime.

In this work, we develop a framework for controlling overdamped dynamical responses. Our approach exploits the fact that overdamped dynamics extremize a quantity known as the Rayleighian [41], which depends on both forces and velocities. Although system trajectories do not generally extremize the time-integrated Rayleighian, the principle of instantaneous extremization provides a natural foundation for constructing approximate learning or adaptation schemes.

We explore two such schemes. The first is a directed aging approach that modifies microscopic parameters to generate a soft mode in the dissipation space, thereby steering the system's dynamical response. The second adapts ideas from equilibrium propagation by applying them to the Rayleighian, yielding local update rules that reduce a chosen dynamical cost function.

We test these approaches numerically in networks of Maxwell viscoelastic elements, which behave elastically at short times and fluid-like at long times. Our goal is to train the finite-rate response, and we demonstrate control over several dynamical properties. In particular, we tune the viscous Poisson's ratio, which governs the response at slow actuation rates. We also train local behaviors, such as responses in which actuation at multiple points produces a prescribed displacement at a distant target. Because elastic and viscous responses depend on distinct microscopic parameters, spring con-

stants and dissipation coefficients, respectively, the fast elastic and slow viscous behaviors can be tuned independently, enabling rate-dependent functionality.

Overall, our results demonstrate that systems composed of many overdamped degrees of freedom can be trained to exhibit programmable dynamical responses. The methods introduced here may be applicable to a broad class of soft and biological materials, and potentially to active or living systems in which local evolution rules are naturally coupled to the dynamics.

II. OVERDAMPED DYNAMICS & THE RAYLEIGHIAN

We consider arbitrary overdamped equations of motion where the velocities are linearly dependent on the forces,

$$\sum_j \eta_{ij} \dot{x}_j = f_i(\{x\}). \quad (1)$$

Here, x_i are the particle positions, f_i are internal or external forces, and η_{ij} is the dissipation matrix, which is symmetric and positive-definite. Symmetry is due to Onsager's reciprocal theorem [42, 43] and positivity ensures that the system cannot spontaneously generate energy.

Methods for controlling the response of elastic or other physical systems often rely on the state being a minimum of some function. For example, in quasistatics, the energy is minimized, and for resistor networks, the dissipated power is minimized. For overdamped dynamics, the state of the system can be defined in either the position of each particle or the velocities, while also specifying the initial conditions. The Rayleighian [41, 43] is a function whose extremum with respect to the velocities yields the equation of motion. It is defined in terms of the dissipation and the rate of change in potential energy,

$$R = \frac{1}{2} \sum_{i,j} \eta_{ij} \dot{x}_i \dot{x}_j - \sum_i f_i(\{x\}) \dot{x}_i. \quad (2)$$

As noted, requiring that $\frac{\partial R}{\partial \dot{x}_i} = 0$ yields the equations of motion. Since the dissipation matrix is positive-definite, the Rayleighian is minimized.

Eq. 2 is remarkably similar to elastic systems, where the energy, in the linear regime, can be expressed in terms of the displacements,

$$U = \frac{1}{2} \sum_{i,j} x_i H_{ij} x_j - \sum_i f_i^{ext} x_i. \quad (3)$$

where $H_{ij} = \frac{\partial^2 U}{\partial x_i \partial x_j}$ is the Hessian and f_i^{ext} is an external force. The Hessian is analogous to the dissipation matrix, the velocities correspond to the displacements and the internal forces correspond to the external forces.

While the momentary evolution is governed by the Rayleighian, the trajectory *does not* extremize the integrated Rayleighian,

$$R_{traj} = \int_{\tau_i}^{\tau_f} d\tau R(\tau). \quad (4)$$

To see this, consider the internal forces (and possibly the dissipation matrix), which depend on the particle positions. The positions implicitly depend on past velocities, $x_i(\tau) = x_i(0) + \int_0^\tau d\tau' \dot{x}(\tau')$ and taking the functional derivative with respect to the velocity at a given time yields additional terms. The integrated Rayleighian is minimized exactly if the forces and the dissipation matrix are constant, and do not depend on positions.

III. MODEL

For concreteness, we test our ideas on a specific model, a disordered network of Maxwell viscoelastic elements [44–46]. The network is a two-dimensional disordered bonded network, where each bond is composed of a spring and a dashpot in series. For convenience, the networks are derived from amorphous packings of spheres where the coordination number is easily tuned [47]. The coordination number is the average number of bonds per node, $Z = \frac{2N_B}{N}$, where N_B is the number of bonds and N is the number of nodes. Here, we consider highly coordinated networks with $Z = \frac{2N_B}{N} \approx 4.52$, far from the threshold needed for rigidity $Z_c = 4$.

As noted, each bond is a spring and dashpot in series. The tension on each bond is

$$t_i = k_i (\ell_i - \ell_{i,0}), \quad (5)$$

where k_i denote the spring constants, ℓ_i are the bond lengths and $\ell_{i,0}$ are the rest lengths. The dashpot accounts for the change in rest length, assumed to be in proportion to the tension on the bonds:

$$\gamma_i \frac{d}{d\tau} \ell_{i,0} = t_i. \quad (6)$$

Here, γ_i are the dissipation coefficients of the dashpots.

In this paper, we focus on the quasistatic regime, where the system is constantly in force balance. This assumes that the time scale for reaching force balance is much smaller than the time scale on which the dashpots evolve. Time is discretized into small intervals, and at each step we compute the tensions, change the rest lengths in accordance with Eq. 6 and then minimize the energy to reach force balance.

For this model, the Rayleighian is given by,

$$R = \frac{1}{2} \sum_i \gamma_i \left(\frac{d\ell_{i,0}}{d\tau} \right)^2 - \frac{d\ell_{i,0}}{d\tau} k_i (\ell_i - \ell_{i,0}) \quad (7)$$

where ℓ_i is determined by the force-balance requirement.

IV. TRAINING RULES

Our goal in this paper is to control trajectories of certain target degrees of freedom. These could be the positions of a specific set of target particles or strain of the

entire system, which we later discuss. To this end, we strain the system at a constant rate and modify γ_i to attain a desired behavior. Based on the analogy to quasistatic mechanics, we employ two methods for adjusting the dissipation coefficients:

(1) **Directed aging approach:** which assumes that internal parameters vary over time due to natural processes, such as aging, plasticity, or damage [18]. This microscopic change to material parameters translates to a change to material properties, including the response to external forcing.

To illustrate how this can be used to tune material properties, we review a rule that was used to tune elastic properties [18]. Consider an elastic system where a bond accumulates damage and weakens over time. That is, we assume that a bond's stiffness decreases at a rate that grows with the tension on that bond,

$$\frac{dk_i}{d\tau} = -r_k k_i (\ell_i - \ell_{0,i})^2. \quad (8)$$

Here, r_k is a rate constant. The tension on a bond depends on the deformation, and therefore, different deformations result in different changes to material properties. For example, under compression, the bonds that counter this deformation weaken at a faster rate, resulting in the decrease of the bulk modulus. This also has the effect of decreasing the Poisson's ratio, since it is a decreasing function of the ratio of the shear modulus to the bulk modulus, G/B [18] (in two dimensions it is given by $\nu_{2d} = \frac{B-G}{B+G}$). Straining under shear, for example, yields a small shear modulus.

For the time being, we do not alter the spring stiffness but rather define a rule that is motivated by Eq. 8. To control the viscous evolution of the Maxwell material, we alter the damping coefficients. Based on the analogy between the Rayleighian on the energy, we assume that the dissipation coefficients degrade at a rate that depends on the creep (plastic strain),

$$\frac{d\gamma_i}{d\tau} = -\gamma_i r_{Age} \left(\frac{d}{d\tau} \ell_{i,0} \right)^2. \quad (9)$$

This evolution is very similar to Eq. 8. Rather than creating a soft direction in energy space, this rule creates a soft direction in the dissipation space. We also include the prefactor γ_i which insures that the γ_i does not become negative.

(2) **Equilibrium propagation:** is a theorem that relates the gradient of an arbitrary cost function to physical measurements [24, 25]. Namely, a physical system can be used to compute a gradient of an arbitrary cost function. The central condition of this theorem is that the system extremizes an energy function, which need not be the physical energy. For the sake of discussion, we focus on quasistatics where the potential energy is minimal.

Equilibrium propagation is a supervised learning rule in which a supervisory signal 'nudges' the system toward the desired behavior. This effect is incorporated through

an additional term in the potential energy, given by the cost function weighted by β :

$$E \rightarrow E + \beta C. \quad (10)$$

Since the cost is minimized at the desired behavior, the additional force 'nudges' the system towards that desired behavior. The gradient of the cost function is given by,

$$\frac{\partial C}{\partial \gamma_i} \approx \frac{1}{\beta} \left[\frac{\partial E^c}{\partial \gamma_i} - \frac{\partial E^f}{\partial \gamma_i} \right]. \quad (11)$$

The superscript c denotes the *clumped state* where the system is nudged towards the desired behavior ($\beta > 0$) due extra potential term. The superscript f denotes the *free state* where there is no additional forcing, $\beta = 0$. This becomes an equality in the limit of $\beta \rightarrow 0$.

To employ this equilibrium propagation in dynamics, we substitute the energy by the Rayleighian,

$$\frac{\partial C}{\partial \gamma_i} \approx \frac{1}{2\beta} \left[\left(\frac{d}{d\tau} \ell_{i,0}^c \right)^2 - \left(\frac{d}{d\tau} \ell_{i,0}^f \right)^2 \right]. \quad (12)$$

Thus, the gradient of a cost function is estimated by the difference in the square of the rate of plastic strain of the dashpot. Note that in comparison to Eq. 9, there is an extra term corresponding to the free state. Next, we assume that γ_i evolves through through gradient descent

$$\frac{d\gamma_i}{d\tau} \propto -\frac{\partial C}{\partial \gamma_i}, \quad (13)$$

where the gradient is estimated using the approximate equilibrium propagation rule.

V. NUMERICAL SIMULATIONS

A. Directed aging for viscous responses

We begin by training viscous responses using the directed aging rule, Eq. 9. Our aim is to reduce the Poisson's ratio to negative values, thereby accessing a regime that is seldom encountered in nature.. We train the system by repeatedly compressing at a constant strain rate, $\dot{\epsilon}_{Age}$, while allowing the dissipation coefficients to evolve through Eq. 9. At each cycle, we reset the system to the same initial conditions. After training, we measure the response to an applied uniaxial strain along the x-axis at a constant rate and measure the resulting strain along the y-axis. Recall, Poisson's ratio is defined as the negative ratio of the strain along the y-axis and the x-axis, $\nu = -\frac{\epsilon_y}{\epsilon_x}$.

The Poisson's ratio after training is shown in Fig. 1(a) at different deformation rates, $\dot{\epsilon}_m$, measured under uniaxial compression. Note that the strain rate at which the response is measured, $\dot{\epsilon}_m$, is generally different from the training strain rate, $\dot{\epsilon}_{Age}$. At fast deformation rates, the response is dominated by the elastic response, which for

this ensemble of networks has a positive Poisson's ratio. At slow deformation rates the Poisson's ratio depends on the strain. For small strains (short times) the deformation is elastic, and the Poisson's ratio is positive. At larger strains, where the viscous relaxation dominates, Poisson's ratio becomes negative. The crossover between the elastic and viscous becomes sharper, and in the limit of vanishing deformation rate, there is a discontinuity in Poisson's ratio at zero strain.

In Fig. 1(b) we plot the Poisson's ratio at the training strain $\epsilon_{Age} = 0.02$, for different values of aging rates, r_{Age} . The response of the system that was not aged ($r_{Age} = 0$), depends very weakly on the strain rate. After training, for large enough aging rates, Poisson's ratio crosses over from negative values at small strain rates to positive values at large strain rates.

We next ask what sets the strain rate of the crossover between the two regimes. For a single dashpot, there is a characteristic strain rate, $\dot{\epsilon} = \epsilon_{Age} \frac{k_i}{\gamma_i}$. For a network of springs, relaxation depends on the interactions of the bonds, which can be solved numerically. There are two simple cases for which the collective evolution can be computed: arranging the bonds either in series or in parallel. Both cases map onto the single bond case with an effective characteristic strain rate, $\epsilon_{Age} \frac{\bar{k}_i}{\gamma_i}$ when in parallel and $\epsilon_{Age} \frac{1/\bar{\gamma}_i}{1/k_i}$ when the bonds are in series. Here, the bar denotes the average over all springs or dashpots, i.e., $\bar{k}_i = \frac{1}{N} \sum_i k_i$. These two values are indicated in Fig. 1(b) by the dashed lines. The crossover occurs between these two values.

We note that $1/\bar{\gamma}_i$ and $1/\gamma_i$ may differ by many orders of magnitude, since the first is dominated by the small values, while the second by the large values. Fig. 1(c) compares $\bar{\gamma}_i$ and $\frac{1}{1/\bar{\gamma}_i}$ as function of time. While $\bar{\gamma}_i$ changes very little, the change to $\frac{1}{1/\bar{\gamma}_i}$ is significant. We also plot in Fig. 1(d) the distribution of $1/\gamma_i$. The distribution for the large r_{Age} approximately is power-law, scaling as $\left(\frac{1}{\gamma_i}\right)^{-3}$. The probability of γ_i at small values can be estimated through a change in variables, yielding $P(\gamma) \propto \gamma$. Namely, the distribution vanishes linearly at small values. Power laws are often associated with criticality. In the appendix VII, we provide a one-dimensional model that yields this scaling. The aging process is self-accelerated (positive feedback). Assuming the tension, t , is fixed, combining the aging rule with the evolution of a dashpot yields $\frac{d\gamma_i}{dt} = -\frac{r_{Age}}{\gamma_i} t^2$. Namely, bonds with small γ_i decrease at a faster rate. This could yield spatial localization of small γ_i , in a crack-like fashion, similar to that occurring in elastic systems [10].

Next, we test the generality of our results and train auxetic responses (negative Poisson's ratio) under expansion. We follow the exact procedure as above. The results, shown in Fig. 2, are similar to those above. Poisson's ratio at fast rates is positive, while at slow rates it can be negative. Interestingly, there is a stronger de-

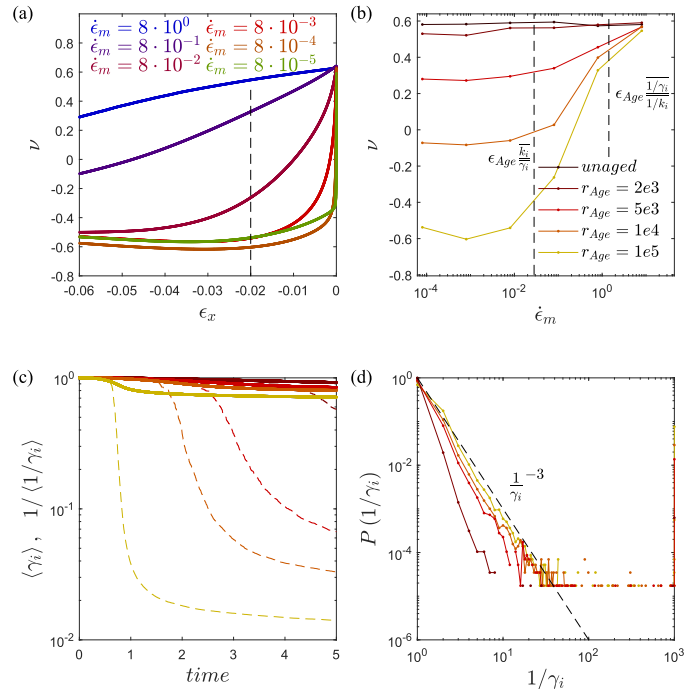


Figure 1. Training with directed aging to control the Poisson's ratio under compression. (a) The Poisson's ratio as a function of strain for different actuation rates. (b) The Poisson's ratio at the training strain as a function of actuation rate, $\dot{\epsilon}_m$. The results are obtained for different training rates. Parameters: $N = 512$, $\dot{\epsilon}_{Age} \gamma_i(0)/k = 8 \cdot 10^{-4}$, $\epsilon_{Age} = 0.02$ and number of training cycles is 10^5 . In (a): $r_{Age} = 10^5$.

pendence on the applied strain. The Poisson's ratio as a function of strain first decreases, reaches a minimum, and then increases. The minimum appears to correspond with the training strain, suggesting that the system encodes a memory of the strain at which it is trained. We also show in Fig.2(b) the Poisson's ratio at the training strain as a function of strain rate. Similarly, to the case of compression, there is a crossover between the quick elastic with a positive Poisson's ratio and the slow viscous responses with a negative Poisson's ratio.

B. Directed aging for local responses

We also explore the possibility of training local responses. We consider N_S source sites that are actuated with the goal of inducing a strain on a single target site. Both the sources and the target are a pair of nearby nodes that are chosen randomly, and the strain is defined as the fractional change in the distance between the nodes. Fig. 3(a) shows an example of the network with the source sites indicated in green and the single target is indicated in red. We train at a strain amplitude of $\epsilon_{Age} = 0.02$ for both the sources and the target; the applied strain is

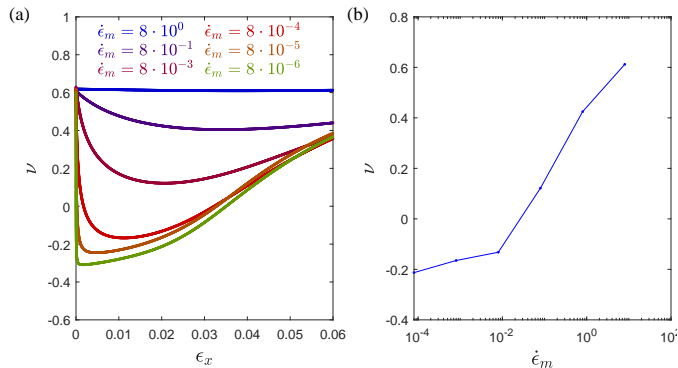


Figure 2. Training with directed aging to control the Poisson's ratio under expansion. (a) The Poisson's ratio as a function of strain (expansion) for different actuation rates. (b) The Poisson's ratio at the training strain as a function of actuation rate. The results are obtained for different training rates. Parameters: $N = 512$, $\dot{\epsilon}_{Age}\gamma_i(0)/k = 4 \cdot 10^{-3}$, $\epsilon_{Age} = 0.02$ and number of training cycles is 10^5 .

either compression or extension, chosen with equal probability.

Fig. 3(b) shows the response at different strain rates to an applied strain on the source sites, ϵ_S . At fast rates, the response is very small and, on average, vanishes. At slow rates, the response approximately follows the desired strain, and the response persists beyond the training strain. Fig. 3(c) shows the strain on the target at the training strain ϵ_{Age} , for different numbers of source sites. The response is the largest when there are sufficient number of source sites. This is consistent with previous findings for other training methods [48]. The difficulty in training local responses is that the elastic (or viscous) Green's function for an applied local force decays quickly with distance from that site. As a result, it is difficult to couple distant sites.

Lastly, we consider the distribution of $1/\gamma_i$, shown in Fig. 3(d). Also here, the distribution scales approximately as $\left(\frac{1}{\gamma_i}\right)^{-3}$. This suggests that this distribution is universal for this training method.

C. Multi-functional responses

Up till now, we have focused on manipulating the slow viscous response, which depends on the dissipation coefficients, γ_i . As noted at fast actuation rates, the response depends on the spring constants, k_i . Since the fast and slow response depends on different sets of parameters, this offers the possibility of modifying the elastic and dissipative responses independently.

To explore the feasibility of tuning these two limits, we train the system using two different training rules. For the sake of this example, we train for a negative Poisson's ratio at fast rates and a positive Poisson's ratio at

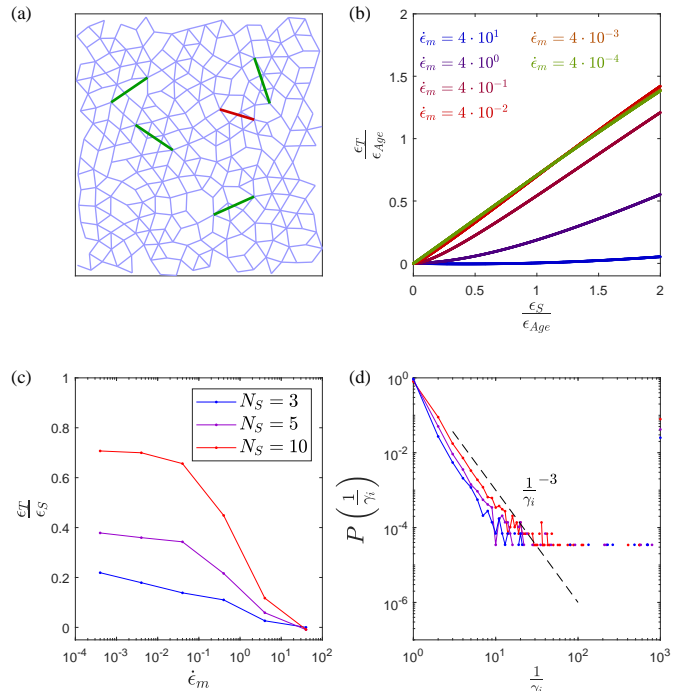


Figure 3. Training local response with directed aging. (a) An illustration of the network with four sources and a single target. (b) The strain on the target as a function of the strain on the source. (c) The average ratio of the strain of the target to the source, as a function of actuation rate for different number of sources. (d) The distribution of the inverse dissipation parameters appears to be power-law, similarly to the results for the Poisson's ratio. Parameters: $N = 256$, $\dot{\epsilon}_{Age}\gamma_i(0)/k = 2 \cdot 10^{-3}$, $\epsilon_{Age} = 0.02$ and number of training cycles is 10^5 . In (b) $N_S = 10$.

slow rates. This is different from above (see Fig. 1(b)) where $\nu > 0$ for fast deformations and $\nu < 0$ for slow deformations. The elastic response is altered by decreasing the spring constants in proportion to the energy on a bond, as defined by Eq. 8. During training for the elastic response, we compress the system isotropically.

After training the elastic response, we then train the slow viscous response by altering the relaxation times of the dashpots in Eq. 9. To increase the Poisson's ratio, we train with a pure shear deformation. We note that the two rules can coincide with each other. Training at fast rates generates large stresses and therefore affects only the spring constants. Training at slow rates is dominated by creep, altering the dissipation coefficients.

Fig. 4(a) shows the Poisson's ratio as a function of applied uniaxial strain. At fast actuation rates, the response has $\nu < 0$, while at slow rates $\nu > 0$ as the system was trained for. Fig. 4 (b) shows ν at the training strain $\epsilon_{Age} = -0.02$, as a function of the deformation rate $\dot{\epsilon}_m$. As shown, there is a crossover between positive and negative Poisson's ratios as a function of actuation rate.

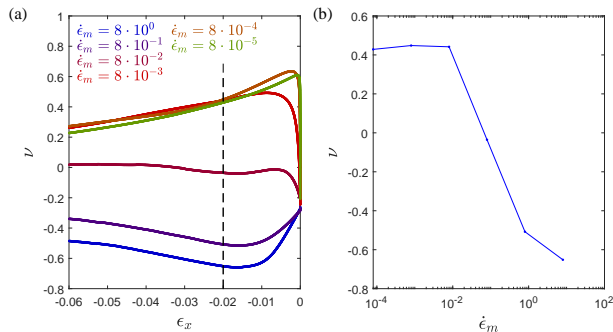


Figure 4. Manipulating simultaneously both the elastic and viscous response using directed aging. (a) The Poisson's ratio as a function of strain for different actuation rates. (b) The Poisson's ratio at the training strain as a function of actuation rate. The results are obtained for different training rates. Simulation parameters: $r_{Age} = 5 \cdot 10^5$, $\epsilon_{Age} = -0.02$, $N = 512$, $\dot{\epsilon}_{train} = 5$, $\dot{\epsilon}_{train} k r_k = 0.01$, $\gamma_0 = 1$, $k_0 = 1$ and number of training cycles is 10^5 .

D. Equilibrium propagation for local responses

Here we train local responses using the equilibrium propagation rule introduced in Eq. 12. As before, we consider several sources and a single target site, which corresponds to pairs of nearby nodes. These are trained with the goal of attaining a desired strain on the target when the sources are strained at a constant rate. We iteratively vary the dissipation coefficients using gradient descent, where in each cycle we begin from the same initial conditions. In each iteration, we strain the system twice, first, in the free state and then in the clumped state. In the free state, we do not apply any forcing to the target, while in the clumped state, we nudge the targets. The small nudging force acts to adjust the distance between the target nodes toward their desired value. Here we choose to take the desired strain to be $\epsilon_T = \epsilon_{Age} (\tau/T)^2$, where T is the actuation time. We choose the quadratic form since it is more consistent with the viscous response. We also limit the maximal and minimal dissipation coefficients.

In Fig. 5(a), we show the error as a function of the number of iterations. The error is defined as the integrated square difference of the target strain rate and the desired strain rate $\frac{1}{T\epsilon_{Age}^2} \int_0^T d\tau (\dot{\epsilon}_T - \dot{\epsilon}_D)^2$. We consider two variations of the nudging force: in the blue curve, the force is proportional to the difference between the velocity in the free state and the desired velocity, while in the red curve, the nudging depends on the difference between the target strain and the desired strain. The nudging force is only approximate and is not derived from the Rayleighian, which is in itself only approximately extremized. For both cases, the error decreases by over an order of magnitude. Fig. 5 shows the strain on the target as a function of the source strain. For both nudging forces, the strain is near the desired values, indicated by

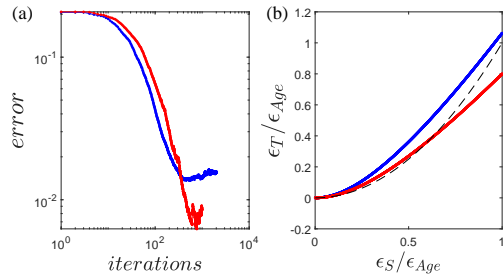


Figure 5. Using equilibrium propagation to train localized response. (a) The error as a function of the number of iterations. (b) The strain on the target as a function of the strain on the source. Blue: We nudge the system with a force that is proportional to the difference in the velocity and the desired velocity ($\dot{\epsilon}_T - \dot{\epsilon}_D$). Red: The nudging depends on the distance between the nodes of the target and their desired value. The dashed line corresponds to the desired strain. Here, $N = 256$, actuation time normalized by dissipation coefficient $\frac{\epsilon_{Age} k}{\epsilon_{Age} \gamma} = 0.04$, $\epsilon_{Age} = 0.02$, $N_S = 5$ and $\beta = 0.001$.

the dashed line.

VI. CONCLUSIONS

In summary, we have shown that the overdamped dynamics of materials can be tuned to allow desired behaviors. We have developed two rules that are derived from the Rayleighian, whose extremum corresponds to the equations of motion. While this is exact at a given point in time, for a trajectory, the integrated Rayleighian is not extremized, and therefore the rules are only approximate. The structure of the Rayleighian is very similar to the elastic energy, where the dissipation matrix corresponds to the elastic Hessian. Based on this analogy, we have derived a directed aging rule where the dashpots degrade as they evolve, creating a soft direction in the dissipation space. A second rule is derived through the equilibrium propagation framework.

We then tested these ideas in a model, consisting of a disordered bonded network where each bond is a spring and dashpot in series. This is the Maxwell model for viscoelastic materials, and its behavior is rate-dependent. On short time scales (fast actuation rates), it is elastic, while on long time scales (slow actuation), it undergoes dissipative flow. The rules are applied to the dissipation coefficients, allowing for tuning the slow relaxation processes. This allows for modifying the Poisson's ratio as well as the local responses that arise due to flow, rather than elasticity. We then studied the feasibility of tuning both the elastic and viscous properties simultaneously. Since the elastic properties depend on the spring constants, they can be modified independently of the dissipation coefficients, which determine the viscous response. As a result, we are able to modify the rate-dependent response, both for fast and slow deformations.

While the current paper has focused on a specific model, controlling the overdamped dynamics could be important for a large set of systems. In materials, this could allow for manipulating the dynamic moduli of viscoelastic solids, the flow of suspensions, and electronic transport. In living systems, on the cellular or molecular scale, dynamics are often overdamped, and the current ideas could be relevant there. Lastly, active systems are also often modeled with first-order equations of motion. Pursuing the line of research we presented, perhaps we could make the methods precise and find applications in both passive and active systems.

ACKNOWLEDGMENTS

This work was supported by the Israel Science Foundation (grant 2385/20) and the Alon Fellowship.

VII. APPENDIX: DISTRIBUTION OF $\frac{1}{\gamma_i}$ IN ONE DIMENSION

In this appendix, we compute the distribution of γ_i for Maxwell elements arranged in series. Since the Maxwell elements are arranged in series, they all experience the same tension, t . Each dashpot evolves in proportion to the tension,

$$\gamma_i \frac{d}{d\tau} \ell_{0,i} = t. \quad (14)$$

We strain the system at a constant rate, which corresponds to increasing the tension at a constant rate r . The tension relaxes due to the extension of the dashpots,

$$\frac{dt}{d\tau} = r + k_{eff} \sum \frac{\ell_{0,i}}{d\tau} \quad (15)$$

$$= r + k_{eff} t \sum \frac{1}{\gamma_i} \quad (16)$$

We will assume that the tension reaches a steady state and that it remains constant. This neglects the effect of the change of γ_i on the tension. The directed aging rule assumes that,

$$\frac{d\gamma_i}{d\tau} = -\gamma_i \left(\frac{d\ell_{0,i}}{d\tau} \right)^2 \quad (17)$$

$$= -\frac{t^2}{\gamma_i}. \quad (18)$$

In the last line, we used the relation between the tension and change in rest length. Alternatively, in term of $\frac{1}{\gamma_i}$,

$$\frac{d}{d\tau} \frac{1}{\gamma_i} = \frac{t^2}{\gamma_i^3}. \quad (19)$$

The distribution of $\mu_i = \gamma_i^{-1}$ obeys the continuity equation,

$$\frac{\partial P(\mu)}{\partial t} = -\frac{\partial}{\partial \mu} (P\mu^3) \quad (20)$$

This equation has no steady state, since γ_i constantly decreases. To estimate the distribution, we add a delta function $\delta(\mu - 1)$ which injects bonds with $\gamma = 1$. The steady state is given by (for $\mu > 1$),

$$P(\mu) = \frac{1}{\mu^3}. \quad (21)$$

This is consistent with the simulations, despite them being in two dimensions.

-
- [1] Masao Doi, Sam F Edwards, and Samuel Frederick Edwards. *The theory of polymer dynamics*, volume 73. Oxford university press, 1988.
- [2] John F Brady, Georges Bossis, et al. Stokesian dynamics. *Annual review of fluid mechanics*, 20(1):111–157, 1988.
- [3] Reza Farhadifar, Jens-Christian Röper, Benoit Aigouy, Suzanne Eaton, and Frank Jülicher. The influence of cell mechanics, cell-cell interactions, and proliferation on epithelial packing. *Current biology*, 17(24):2095–2104, 2007.
- [4] Dapeng Bi, Xingbo Yang, M Cristina Marchetti, and M Lisa Manning. Motility-driven glass and jamming transitions in biological tissues. *Physical Review X*, 6(2):021011, 2016.
- [5] Tamás Vicsek, András Czirók, Eshel Ben-Jacob, Inon Cohen, and Ofer Shochet. Novel type of phase transition in a system of self-driven particles. *Physical review letters*, 75(6):1226, 1995.
- [6] Sadjad Arzash, Indrajit Tah, Andrea J Liu, and M Lisa Manning. Rigidity of epithelial tissues as a double optimization problem. *Physical Review Research*, 7(1):013157, 2025.
- [7] Samar Alqatari and Sidney R Nagel. Evolutionary pathways in epistatic mechanical networks. *Proceedings of the National Academy of Sciences*, 123(5):e2505183123, 2026.
- [8] Ole Sigmund and Salvatore Torquato. Composites with extremal thermal expansion coefficients. *Applied Physics Letters*, 69(21):3203–3205, 1996.
- [9] Katia Bertoldi, Vincenzo Vitelli, Johan Christensen, and Martin Van Hecke. Flexible mechanical metamaterials. *Nature Reviews Materials*, 2(11):1–11, 2017.

- [10] Carl P Goodrich, Andrea J Liu, and Sidney R Nagel. The principle of independent bond-level response: Tuning by pruning to exploit disorder for global behavior. *Physical review letters*, 114(22):225501, 2015.
- [11] Jason W Rocks, Nidhi Pashine, Irmgard Bischofberger, Carl P Goodrich, Andrea J Liu, and Sidney R Nagel. Designing allostery-inspired response in mechanical networks. *Proceedings of the National Academy of Sciences*, 114(10):2520–2525, 2017.
- [12] Mengjie Zu, Aayush Desai, and Carl P Goodrich. Fully independent response in disordered solids. *Physical Review Letters*, 134(23):238201, 2025.
- [13] Chad A Mirkin, Robert L Letsinger, Robert C Mucic, and James J Storhoff. A dna-based method for rationally assembling nanoparticles into macroscopic materials. In *Spherical Nucleic Acids*, pages 3–11. Jenny Stanford Publishing, 2020.
- [14] Sharon C Glotzer and Michael J Solomon. Anisotropy of building blocks and their assembly into complex structures. *Nature materials*, 6(8):557–562, 2007.
- [15] Angus McMullen, Miranda Holmes-Cerfon, Francesco Sciortino, Alexander Y Grosberg, and Jasna Brujic. Freely jointed polymers made of droplets. *Physical review letters*, 121(13):138002, 2018.
- [16] Stefano Sacanna and David J Pine. Shape-anisotropic colloids: Building blocks for complex assemblies. *Current opinion in colloid & interface science*, 16(2):96–105, 2011.
- [17] Jason W Rocks, Henrik Ronellenfitsch, Andrea J Liu, Sidney R Nagel, and Eleni Katifori. Limits of multifunctionality in tunable networks. *Proceedings of the National Academy of Sciences*, 116(7):2506–2511, 2019.
- [18] Nidhi Pashine, Daniel Hexner, Andrea J Liu, and Sidney R Nagel. Directed aging, memory, and nature’s greed. *Science advances*, 5(12):eaax4215, 2019.
- [19] Hriday Kedia, Deng Pan, Jean-Jacques Slotine, and Jeremy L England. Drive-specific selection in multistable mechanical networks. *The Journal of Chemical Physics*, 159(21), 2023.
- [20] Edward YX Ong, Anna R Barth, Navneet Singh, Meera Ramaswamy, Abhishek Shetty, Bulbul Chakraborty, James P Sethna, and Itai Cohen. Jamming memory into acoustically trained dense suspensions under shear. *Physical Review X*, 14(2):021027, 2024.
- [21] Chukwunonso Arinze, Menachem Stern, Sidney R Nagel, and Arvind Murugan. Learning to self-fold at a bifurcation. *Physical Review E*, 107(2):025001, 2023.
- [22] Varda F Hagh, Sidney R Nagel, Andrea J Liu, M Lisa Manning, and Eric I Corwin. Transient learning degrees of freedom for introducing function in materials. *Proceedings of the National Academy of Sciences*, 119(19):e2117622119, 2022.
- [23] Savannah D Gowen, Elina Ghimire, Charlie A Lindberg, Ingrid S Appen, Stuart J Rowan, and Sidney R Nagel. Training and retraining liquid crystal elastomer meta-materials for pluripotent functionality. *Proceedings of the National Academy of Sciences*, 122(29):e2504304122, 2025.
- [24] Benjamin Scellier and Yoshua Bengio. Equilibrium propagation: Bridging the gap between energy-based models and backpropagation. *Frontiers in computational neuroscience*, 11:24, 2017.
- [25] Menachem Stern, Daniel Hexner, Jason W Rocks, and Andrea J Liu. Supervised learning in physical networks: From machine learning to learning machines. *Physical Review X*, 11(2):021045, 2021.
- [26] Vidyesh Rao Anisetti, Benjamin Scellier, and Jennifer M Schwarz. Learning by non-interfering feedback chemical signaling in physical networks. *Physical Review Research*, 5(2):023024, 2023.
- [27] Menachem Stern and Arvind Murugan. Learning without neurons in physical systems. *Annual Review of Condensed Matter Physics*, 14(1):417–441, 2023.
- [28] Vidyesh Rao Anisetti, Ananth Kandala, Benjamin Scellier, and JM Schwarz. Frequency propagation: Multi-mechanism learning in nonlinear physical networks. *Neural Computation*, 36(4):596–620, 2024.
- [29] Lauren E Altman, Menachem Stern, Andrea J Liu, and Douglas J Durian. Experimental demonstration of coupled learning in elastic networks. *Physical Review Applied*, 22(2):024053, 2024.
- [30] Roie Ezraty, Menachem Stern, and Shmuel M Rubinstein. Harnessing intuitive local evolution rules for physical learning. *Physical Review E*, 113(2):025304, 2026.
- [31] Ben-Haim Eran, Givli Sefi, Or Yizhar, and Gat D Amir. Multistable physical neural networks. *Advanced Intelligent Systems*, page 2400694, 2025.
- [32] Sadjad Arzash and Shiladitya Banerjee. Learning epithelial elasticity via local tension remodeling. *bioRxiv*, pages 2025–12, 2025.
- [33] Yao Du, Ryan van Mastrigt, Jonas Veenstra, and Corentin Coulais. Metamaterials that learn to change shape. *arXiv preprint arXiv:2501.11958*, 2025.
- [34] Vishal P Patil, Ian Ho, and Manu Prakash. Self-learning mechanical circuits. *arXiv preprint arXiv:2304.08711*, 2023.
- [35] Jack Kendall. A gradient estimator for time-varying electrical networks with non-linear dissipation. *arXiv preprint arXiv:2103.05636*, 2021.
- [36] Victor Lopez-Pastor and Florian Marquardt. Self-learning machines based on hamiltonian echo backpropagation. *Physical Review X*, 13(3):031020, 2023.
- [37] Guillaume Pourcel, Debabrota Basu, Maxence Ernoult, and Aditya Gilra. Lagrangian-based equilibrium propagation: generalisation to arbitrary boundary conditions & equivalence with hamiltonian echo learning. *arXiv preprint arXiv:2506.06248*, 2025.
- [38] Guillaume Pourcel and Maxence Ernoult. Learning long range dependencies through time reversal symmetry breaking. *arXiv preprint arXiv:2506.05259*, 2025.
- [39] Serge Massar. Equilibrium propagation for learning in lagrangian dynamical systems. *Physical Review E*, 112(3):035304, 2025.
- [40] Marc Berneman and Daniel Hexner. Equilibrium propagation for dissipative dynamics. *arXiv preprint arXiv:2506.20402*, 2025.
- [41] John William Strutt Baron Rayleigh. *Some general theorems relating to vibrations*. London Mathematical Society, 1873.
- [42] Lars Onsager. Reciprocal relations in irreversible processes. i. *Physical review*, 37(4):405, 1931.
- [43] Masao Doi. Onsager principle in polymer dynamics. *Progress in Polymer Science*, 112:101339, 2021.
- [44] James Clerk Maxwell. Iv. on the dynamical theory of gases. *Philosophical transactions of the Royal Society of London*, (157):49–88, 1867.
- [45] Roderic S Lakes. *Viscoelastic materials*. Cambridge university press, 2009.

- [46] Alessio Zaccone. General theory of the viscosity of liquids and solids from nonaffine particle motions. *Physical Review E*, 108(4):044101, 2023.
- [47] Corey S O’hern, Leonardo E Silbert, Andrea J Liu, and Sidney R Nagel. Jamming at zero temperature and zero applied stress: The epitome of disorder. *Physical Review E*, 68(1):011306, 2003.
- [48] Daniel Hexner, Andrea J Liu, and Sidney R Nagel. Periodic training of creeping solids. *Proceedings of the National Academy of Sciences*, 117(50):31690–31695, 2020.